Cell. Mol. Biol. (ISSN: 1165-158X)

Journal Homepage: www.cellmolbiol.org

Cellular and Molecular Biology

Original Article

M2 macrophages regulate KDM6B/PFKFB2 metabolic reprogramming of cervical squamous cell carcinoma through CXCL1

Jing Yu[1], Longzhang Huang[2,*], Lihua Cao[3]

[1] *Department of Gynecological Oncology, Jiujiang Third People's Hospital, Jiujiang, Jiangxi 332000, China*
[2] *Department of Oncology, Jiujiang Third People's Hospital, Jiujiang, Jiangxi 332000, China*
[3] *Department of Nursing, Jiujiang Third People's Hospital, Jiujiang, Jiangxi 332000, China*

Article Info

Article history:

Received: January 16, 2024
Accepted: April 13, 2024
Published: June 30, 2024

Use your device to scan and read the article online

Abstract

Macrophages in the tumor microenvironment can polarize into M1 or M2 forms, with M2 macrophages (M2φ) promoting tumor growth and metastasis in cervical squamous cell carcinoma (CESC). This study explored the effects of M2φ on CESC metabolic reprogramming both in vitro and in vivo. Results showed that M2φ secreted CXCL1, which significantly increased CESC migration and metabolic regulation. Further experiments revealed that CXCL1 upregulated KDM6B to enhance PFKFB2 transcriptional activity, thus regulating CESC glucose metabolism. Transcriptome sequencing screened 5 upregulated genes related to glycolysis, with PFKFB2 showing the most significant increase in cells treated with rCXCL1. Dual-luciferase reporter assay confirmed that rCXCL1 enhances PFKFB2 transcriptional activity. Bioinformatics analysis revealed a high correlation between expressions of KDM6B and PFKFB2 in CESC. Mechanistic experiments demonstrated that KDM6B inhibited H3K27me3 modification to activate PFKFB2 transcriptional expression. In conclusion, M2φ secreted CXCL1 to promote CESC cell migration and invasion, and CXCL1 activated KDM6B expression in CESC cells, inhibiting H3K27 protein methylation modification, and enhanced PFKFB2 transcriptional activity to regulate CESC glucose metabolism. These results provided new insights into the complex interplay between the immune system and cancer metabolism, which may have broader implications for understanding and treating other types of cancer.

Keywords: Cervical squamous cell carcinoma, Glycolysis, CXCL1, PFKFB2, Macrophages.

1. Introduction

Cervical squamous cell carcinoma (CESC) initiates in the squamous cells, which are located in the surface of the cervix [1]. It accounts for 80-90% of total cases and is the most common type of cervical cancer [2]. Macrophages are one of the most abundant stromal cells in microenvironment and can participate in tumor-related biological processes in two forms of polarization, M1 or M2 [3]. Multiple studies related to CESC have shown that M2-polarized macrophages (M2φ) promote tumor growth and metastasis [4]. However, there is less research on the effect of M2φ on CESC metabolic reprogramming.

Chemokines are important substances for communication and information transfer between macrophages and other cells in the microenvironment [5, 6]. In our research, chemokines in M2φ lysate were detected via array analysis, which revealed significant differentiation in expression of C-X-C Motif Chemokine Ligand 1 (CXCL1) between THP-1 and M2φ. In 2021, Wu et al. discovered that CXCL1 was upregulated in CESC tissues than in the normal ones [7]. However, its actual medical significance remained to be explored in a large space.

Cancer cells exhibit a metabolic adaptation known as the Warburg effect, characterized by an elevated rate of glycolysis, enabling them to thrive and proliferate in the hypoxic microenvironment typical of neoplastic tissues [8, 9]. In our bioinformatics analysis, presented as heat map, 6-Phosphofructo-2-Kinase/Fructose-2,6-Biphosphatase 2 (PFKFB2) ranking the most differentially expressed genes that related to glycolysis in CESC cells after rCXCL1 treatment. In pancreatic cancer cells, PFKFB2 is essential for steady-state glycolytic activity, F2,6BP levels, and proliferation of pancreatic adenocarcinoma cells [10, 11]. However, the deep correlation between PFKFB2 and CESC and the underlying regulatory axis was not mentioned in previous work.

Positive correlation between demethylase Lysine (K)-specific demethylase 6B (KDM6B) and PFKFB2 was determined via GEPIA website. It has been found that KDM6B inhibits breast cancer metastasis via interacting with exosomes [12, 13]. It has been also proven to promote lung metastasis of osteosarcoma [14] and stemness of human mesenchymal stem cells via regulating sodium lactate [15].

In summary, we hypothesized that KDM6B/PFKFB2/CXCL1 axis may be involved in the metabolic process of

* Corresponding author.
E-mail address: 879544141@qq.com (L. Huang).
Doi: http://dx.doi.org/10.14715/cmb/2024.70.6.13

CESC induced by M2φ, which would shed light on the complex interplay between immune cells and cancer cells, and provide new insights into the mechanisms underlying CSCC development and progression.

2. Materials and methods

2.1. Macrophage polarization and conditioned medium preparation

M2φ were generated by initially subjecting THP-1 cells to phorbol 12-myristate 13-acetate (PMA, 16561-29-8, Sigma-Aldrich, USA) at a concentration of 320 nmol/L for a period of 12 hours, followed by subsequent culturing with a combination of 100 nmol/L PMA, as well as 20 ng/mL IL-4 (SRP4137, Sigma-Aldrich, USA) and 20 ng/mL IL-13 (SRP3274, Sigma-Aldrich, USA) for an additional duration of 48 h. M2φ cells were cultured in medium without serum for 24 hours, followed by centrifugation at 10,000 rpm for 5 minutes. The resulting supernatant was collected as M2φ-CM and stored at -80°C.

2.2. Cell culture

THP-1 (TIB-202), SiHa (HTB-35) and C33A (HTB-31) cells were all purchased from ATCC (USA). THP-1 cells were cultivated in RPMI-1640 medium + 10% FBS (30-2001, ATCC, USA). SiHa and C33A cells were cultured in MEM medium +10% FBS (30-2003, ATCC, USA). All cells were set in an environment with 95% air and 5% CO_2 at 37°C. After 3 days of culture, the culture media was replaced with M2 macrophage conditioned medium (M2φ-CM) or control media (RPMI + 5% FBS) and co-cultivated for 24 h. CXCL1 antibody (CXCL1 Ab, 250 ng/mL) or was used to treat cells for CXCL1 inhibition. Recombinant CXCL1 (rCXCL1, 100 μg/mL, 275-GR, Bio-techne, China) was used to increase the expression of CXCL1.

2.3. Cell transfection

Sh-NC/PFKFB2 and sh-NC/KDM6B were designed and synthesized by VectorBuilder (China). All vectors were transfected into NMCMs using Lipofectamine 2000 transfection reagents (11668019, Invitrogen, USA).

2.4. Cell Counting Kit-8 (CCK-8) assay

SiHa and C33A cells were seeded in 96-well plates at 1×10^4 cells/well. After that, 10 μl of the CCK-8 solution (Dojindo) was added to each well for a 1h-incubation at 37°C in a humidified incubator with 5% CO_2. Reagents were all from Cell Counting Kit 8 (ab228554, Abcam, UK). The absorbance was measured at 450 nm using microplate reader.

2.5. Wound healing assay

Initially, a 500 μL cell suspension with a concentration of 1.0×10^6 cells/mL was prepared and dispensed into individual wells. Aseptic forceps were utilized to gradually extract the insert from the well of the plate. After discarding non-viable cells and debris through washing, fresh media supplemented with FBS was introduced to facilitate further cell culture. Subsequently, the wound was monitored via light microscopy, and the rate of cellular migration was quantified. The experimental operations were conducted using CytoSelect 24-well Wound Healing Assay kit (MBS168434-6, Biotrend, Germany).

2.6. Transwell assay

The Transwell assay was performed utilizing the CytoSelect™ 24-Well Cell Invasion Assay kit (CBA-110, AmyJet, China) to evaluate cellular invasion. For the migration assay, cells were placed onto the upper chamber of the 8 μm-membrane (which was coated with an additional 20 μL of extracellular matrix gel (Sigma, USA) for the invasion assay) and incubated at 37°C for 10 min. Subsequently, 10% FBS and 500 μL of medium were added to the lower chamber using a pipette. Following 24 hours of incubation, crystal violet staining (ab246820, Abcam, UK) was carried out for 30 minutes at room temperature, and the cells were observed under a microscope (Nikon, Japan).

2.7. Enzyme-linked immunosorbent assay (ELISA)

Human Lactic Acid ELISA Kit (MBS725192), Human Glucose ELISA Kit (MBS7254179), and Human Adenosine triphosphate (ATP) ELISA Kit were all purchased from (MyBioSource, USA). Human CXCL1/GRO alpha DuoSet ELISA (DY275, Bio-techne, China) was used for detection of CXCL1. All procedures were in accordance with guidelines. The results were read at 450 nm immediately and calculated.

2.8. Extracellular acidification rate (ECAR) assay

The ECAR was determined using the Extracellular Acidification Rate Assay Kit (BB-48311, Bestbia, China) in a 24-well plate. The cells were initially seeded and incubated overnight. After 2 times washing using medium containing 2 Mm glutamine at a concentration of 500 μL/well. After a 1-hour incubation period without CO_2, glucose (10 mM), oligomycin (1 μM), and 2-DG (100 mM) were added. The Seahorse XFe24 extracellular flux analyzer (Seahorse Bioscience, Billerica, MA, USA) was utilized to quantify the ECAR.

2.9. Cytokine array detection

Proteome Profiler Human Chemokine Array Kit (ARY017, Bio-techne, China) was used for this detection. In brief, supernatants derived from THP-1 cells and M2φ were harvested. The antibody array membranes were pretreated with 5% bovine serum albumin (BSA) and subsequently co-cultured with the supernatants overnight at 4 °C. Following three times washing, the membranes were treated with biotinylated antibody cocktail. Signals were amplified using horseradish peroxidase-streptavidin. ECL Advance reagent was used for visualization and ImageLab software was for quantification.

2.10. RNA sequencing (RNA-seq)

RNA-seq was employed to investigate the differential expression of genes related to glycolysis in CESC cells treated with rCXCL1 or negative control. Prior to RNA extraction, the cells were washed thrice with phosphate-buffered saline (PBS) and total RNA was extracted using TRIzol Reagent. Subsequently, RNA-seq was performed at BGI Genomics (Wuhan, China) to analyze the transcriptome of the samples. Raw reads were sequenced and subjected to quality control (QC) procedures, following which high-quality reads were mapped to a reference genome. Gene quantitative analysis was conducted, and gene expression levels were subjected to various analyses, including principal component and correlation analy-

sis as well as differential gene screening. The fragments per kilobases per million fragments method (FPKM) was used to assess the expression level and determine the fold change between the samples. Differential expression genes (DEGs) were identified with a log2 (fold change) > 1 or log2 (fold change) < −1 and statistical significance (p-value < 0.05).

2.11. Bioinformatics analysis

UALCAN (https://ualcan.path.uab.edu/) is a web portal for analyzing cancer transcriptome data, providing gene expression profiling, survival analysis, and pathway analysis and was used to detect expression of PFKFB2 in CESC tissues. GEPIA (http://gepia.cancer-pku.cn/) is a website collecting expression data of RNA sequencing from tumor/normal patients, providing customizable and interactive charts and tables for gene expression analysis, and was used to analyze the correlation between KDM6B and PFKFB2.

2.12. Quantitative reverse transcription polymerase chain reaction (qRT-PCR)

The RNA extraction procedure employed TRIzol® Reagent (15596018, ThermoFisher, USA) and subsequent reverse transcription was carried out using the AffinityScript cDNA Synthesis Kit (200436, Agilent, USA). The PCR process was conducted using SYBR™ Green HiScript® III RT SuperMix (R323, Vazyme, China) with three replicates per cycle. The $2^{-\Delta\Delta CT}$ method was used to analyze the PCR results. The primers were as follows: PFKFB2: F: 5'-AGAAATGTTCATGGGCCTC-3', R: 5'-GTTTCTTGGACACGTAGGT-3'; KDM6B: F: 5'-TTTCATACTGGCTCCTGCC-3', R: 5'-GTTCCGTTTGTGCTCAAGG-3'.

2.13. Western blot (WB)

The cells were subjected to PBS washing and subsequent lysis using Total Protein Extraction Kit (2140, Millipore, China). The protein lysate was agitated intermittently on ice at 5-minute intervals. Protein concentration was determined using the Pierce™ BCA Protein Assay Kit (23225, ThermoFisher, USA), and equivalent protein amounts were loaded into each lane of SDS-PAGE and then transferred to PVDF membranes (88518, ThermoFisher, USA). After membrane-blocking, primary antibodies were incubated with the membranes overnight at 4°C and then removed. The PVDF membranes were further treated with secondary antibodies (ab7090, 1:1000, Abcam, UK) at 37°C for 1 hour. Finally, the protein bands and results were visualized using the enhanced chemiluminescence (ECL) Fluorescent Western blotting kit (Advansta, Menlo Park, USA). The primary antibodies were as follows: anti-PFKFB2 (ab234865, 1/1000, Abcam, UK); anti-KDM6B (ab169197, 1/1000, Abcam, UK); anti-H3K27me3 (ab6002, Abcam, UK).

2.14. Dual-luciferase reporter assay

The promoter sequence of PFKFB2 was subcloned into the pmirGLO vector, which was subsequently transfected into SiHa cells from two distinct groups: rCXCL1 and Ctrl. Lipofectamine 3000 was utilized as the transfection agent. The analysis of relative luciferase activities was conducted at 48 hours post-transfection using the Dual-Luciferase Reporter Detection System (Promega).

2.15. Chromatin Immunoprecipitation (ChIP) assay

Reagents used were from ChIP Assay Kit (17-295, Millipore, USA). Samples were prepared in strict accordance with the manufacturer's instructions and subjected to immunoprecipitation with either 5 μg of anti-IgG (ab76149, Abcam, USA) or anti-H3K27me3 (ab6002, Abcam, USA) antibodies overnight at 4℃. The immunoprecipitated complex was further enriched with 50 ml of Protein A + G Agarose, and incubated at 4℃ for 60 min, followed by centrifugation at 1000 g for 1 min. The resulting precipitate was extensively washed and subsequently analyzed by PCR.

2.16. Animal model

A group of female BALB/c nude mice aged between 5-7 weeks (n = 10) were subcutaneously injected with either 4×10^6 SiHa, SiHa + M2φ, or SiHa + M2φ/sh-CXCL1 (or SiHa transfected with sh-NC, sh-KDM6B-1 or sh-KDM6B-1 + PFKFB2) in the right armpit region. Subsequent to cell injection, tumor volume was measured on the 7th, 14th, 21st, and 28th days utilizing the formula V = length × width^2/2. Following a 5-week period post-cell injection, mice were euthanized, and tumor tissues were extracted and weighed.

2.17. Immunohistochemistry (IHC) assay

IHC was performed as previously described [16]. Primary antibodies against Ki67 (ab15580), KDM6B (ab38113), PFKFB2 (ab234865) and CXCL1 (ab269939) were purchased from Abcam (UK). Tumor samples were fixed, dehydrated, embedded and cut into 5 micron thick sections. The sections were deparaffinized using xylene and rehydrated using 70% ethanol solutions. After antigen retrieval and blocking, primary antibodies were diluted and incubated with tissue sections for 1 h at room temperature. Secondary antibody (ab288151, Abcam, UK) was added for another 1 h at room temperature. eBioscience™ DAB Advanced Chromogenic Kit (8801-4965-72, Invitrogen, USA) was used for visualization.

2.18. Statistical analysis

The data was processed with the aid of SPSS 22.0. Descriptive statistics were employed to report variable data in terms of mean ± standard deviation (SD). One-way ANOVA and student's t-test were utilized to compare group differences. The statistical significance level was set at $P < 0.05$.

3. Results

3.1. M2 macrophages regulated the metabolism in CESC cells

SiHa and C33A cells were treated with M2φ-CM to assess the regulatory effect of M2 macrophage (Figure 1A). Both cell lines showed significantly increased viability in M2φ-CM groups, as compared to Ctrl groups (Figure 1B). Higher migration rate was determined in M2φ-CM group than in Ctrl group via wound healing assay (Figure 1C). Transwell assay detected both increased migration and invasion cells in M2φ-CM groups, as compared to Ctrl groups (Figure 1D). Meanwhile, glucose uptake, lactate and ATP levels were all boosted by M2φ-CM in SiHa and C33A cells, assessed by ELISA (Figure 1E-G). Higher ECAR levels remained throughout the whole 120 min of observation in M2φ-CM groups than in Ctrl groups (Figure 1H). These results suggested that M2 macrophages

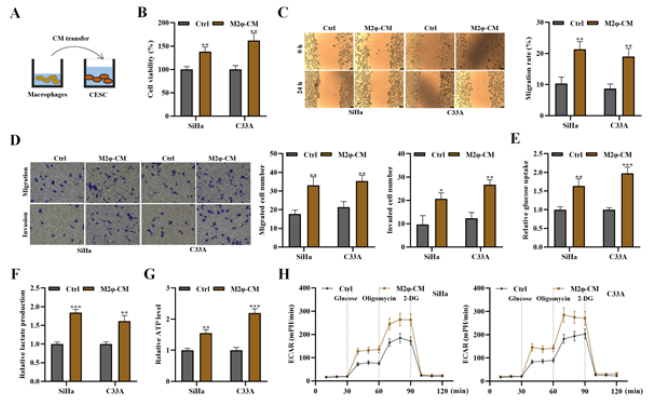

Fig. 1. (A) Procedure of treatment of CESC cells with M2φ-CM. (B) Cell viability of SiHa and C33A cells treated with Ctrl/M2φ-CM, detected by CCK8 assay. (C) Migration rate of wounded SiHa and C33A cells treated with Ctrl/M2φ-CM, assessed by wound healing assay. (D) Number of migrated and invaded cells from Ctrl/M2φ-CM group, assessed by transwell assay. (E-G) Levels of glucose uptake, lactate and ATP in cells from Ctrl/M2φ-CM group, assessed by ELISA. (H) ECAR in cells from Ctrl/M2φ-CM group.

promoted proliferation and migration of CESC cells and regulated glycometabolism.

3.2. CXCL1 secreted by M2 macrophages mediated glucose metabolism in CESC cells

Chemokine in CESC cell lysate was detected via array analysis, which showed significant differentiation in CXCL1 expression between THP-1 cells and M2 macrophages (Figure 2A). ELISA confirmed relatively high level of CXCL1 in M2 macrophages, as compared to that in THP-1 cells (Figure 2B). Same trend of increased CXCL1 expression was also demonstrated in SiHa and C33A cells co-cultured with M2φ-CM (Figure 2C). Therefore, co-culture system of SiHa and C33A cells and M2φ-CM was treated with CXCL1 Ab for further validation. Compared to M2φ-CM group, M2φ-CM + CXCL1 Ab group manifested relatively suppressed viability and decreased number of migrated and invaded cells (Figure 2D-F), suggesting M2 macrophages regulated tumor progression via secreting CXCL1. Furthermore, CESC cells were treated with rCXCL1, and the positive correlation between concentration of rCXCL1 and levels of glucose uptake, lactate, ATP and ECAR was observed (Figure 2G-J), indicating that the effect of CXCL1 was concentration-dependent.

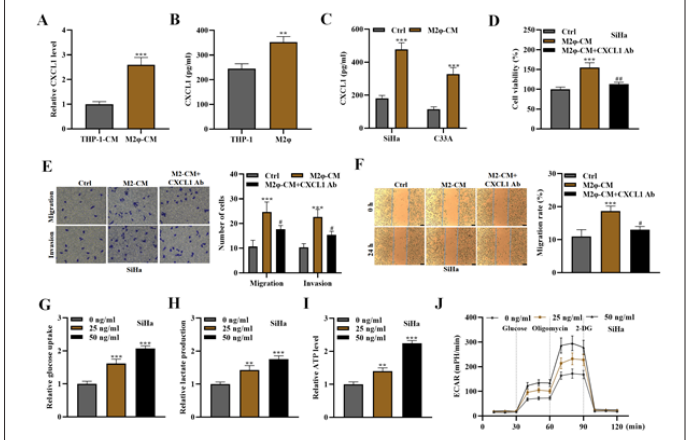

Fig. 2. (A) Relative level of chemokine in supernatant of CESC cells, detected via array analysis. (B) CXCL1 content in supernatant of THP-1 and M2 macrophages, was detected via ELISA. (C) CXCL1 content in Ctrl/M2φ-CM group, detected via ELISA. (D) Proliferation of Ctrl/M2φ-CM/M2φ-CM + CXCL1 Ab group, assessed by CCK-8 assay. (E) Invasion and migration of Ctrl/M2φ-CM/M2φ-CM + CXCL1 Ab group, assessed by transwell assay. (F) Migration rate of Ctrl/M2φ-CM/M2φ-CM + CXCL1 Ab group, assessed by wound healing assay. (G-I) Levels of glucose uptake, lactate and ATP in SiHa and C33A cells treated with different concentrations of rCXCL1, assessed by ELISA. (J) ECAR in SiHa and C33A cells treated with different concentrations of rCXCL1.

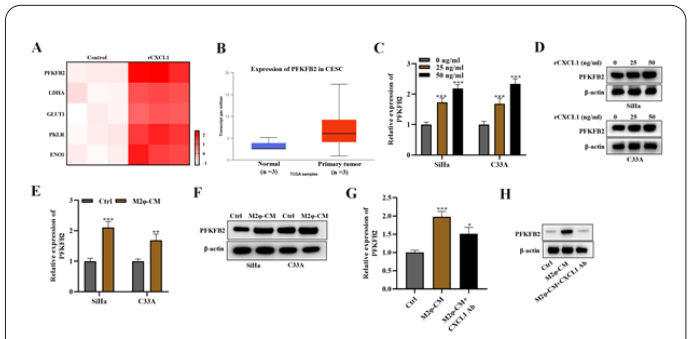

Fig. 3. (A) Differentially expressed genes related to glycolysis in CESC cells treated with rCXCL1. (B) PFKFB2 expression in tissues from normal/CESC patients. (C-D) PFKFB2 expression cells treated with rCXCL1 at different concentrations, were detected via qRT-PCR and WB. (E-F) PFKFB2 expression in cells from M2φ-CM/Ctrl group, detected via qRT-PCR and WB. (G-H) PFKFB2 expression in cells treated with Ctrl/M2φ-CM/M2φ-CM + CXCL1 Ab group, detected via qRT-PCR and WB

3.3. Chemokine CXCL1 upregulated the expression of PFKFB2

As shown in heat map, five differentially expressed genes related to glycolysis were screened via RNA-seq, with PFKFB2 ranking the most difference after rCXCL1 treatment (Figure 3A). PFKFB2 showed significantly higher expression in primary tumor patients (n=305) than in normal ones (n=3), as analyzed by UALCAN website (Figure 3B). In SiHa and C33A cells treated with rCXCL1, its expression was upregulated as the concentration of rCXCL1 increased (Figure 3C-D). In SiHa and C33A cells treated with M2φ-CM, PFKFB2 expression was increased, compared to that in Ctrl group (Figure 3E-F) and such increase was relatively reversed by additional CXCL1 Ab (Figure 3G-H). These results suggested that chemokine CXCL1 upregulated the expression of PFKFB2.

3.4. KDM6B promoted the transcription of PFKFB2 by modulating H3K27

No significant difference in PFKFB2 mRNA expression was detected in SiHa cells from Ctrl/rCXCL1 group (Figure 4A). Relative luciferase activity showed no significant changes between Vector and PFKFB2 promoter groups and remarkable increase in rCXCL1 group, compared to Ctrl group (Figure 4B), suggesting that rCXCL1 activated the transcriptional activity of PFKFB2 without influencing its mRNA stability. Positive correlation between demethylase KDM6B and PFKFB2 was determined via GEPIA website (Figure 4C). qRT-PCR and WB were used for confirmation, which showed that in SiHa and C33A cells

treated with rCXCL1, expression of KDM6B was upregulated compared to the negative control (Figure 4D-E). Therefore, sh-KDM6B was transfected in SiHa and C33A cells (interference efficiency shown Figure 4F). PFKFB2 expression was inhibited by sh-KDM6B, assessed by qRT-PCR and WB (Figure 4G-H). In SiHa and C33A cells transfected with sh-KDM6B, H3K27me3 expression was significantly increased (Figure 4I). ChIP results indicated substantial enrichment of PFKFB2 promoter precipitated by anti-H3K27me3 (Figure 4J), which was further enriched in sh-KDM6B groups (Figure 4K), suggesting KDM6B facilitated the binding of PFKFB2 promoter and H3K27me3, thus to inhibit the transcription of PFKFB2.

3.5. CXCL1/KDM6B/PFKFB2 axis promoted CESC progression in vivo

In vivo, the SiHa + M2φ group largely boosted tumor progression, with its volume and weight increased, compared to the Ctrl group, and SiHa + M2φ/sh-CXCL1 group significantly reversed this effect, compared to the SiHa + M2φ group (Figure 5A-B). IHC results detected higher expression of KDM6B and PFKFB2 in SiHa + M2φ group than in Ctrl group, and lower one in SiHa + M2φ/sh-CXCL1 group than in SiHa + M2φ group (Figure 5C). Moreover, in mice subcutaneously injected with SiHa cells which transfected with sh-NC, sh-KDM6B-1 or sh-KDM6B-1 + PFKFB2, the inhibited tumor progression and expression of KDM6B and PFKFB2 in sh-KDM6B-1 group was then observed promoted in sh-KDM6B-1 + PFKFB2 group, with decreased volume and weight of tumor again increased (Figure 5D-F). These results suggested that KDM6B regulates CESC progression via PFKFB2.

4. Discussion

Synthesized by tissue macrophages and functioning as neutrophil chemoattractants, CXCL1 was found to control the early stage of neutrophil recruitment during tissue inflammation [17]. It was dysregulated in immune escape and lung metastasis of breast cancer [18] and pancreatic cancer [19]. However, its expression in polarized macrophages has never been explored in CESC. In our research, ELISA confirmed relatively high level of CXCL1 in M2 macrophages or CESC cells co-cultured with M2φ-CM. Moreover, the addition of CXCL1 Ab to CESC cells co-cultured with M2φ-CM significantly suppressed viability, invasion and migration of cells, suggesting M2φ regulated tumor progression via secreting CXCL1 in a concentration-dependent manner.

It was assessed in colorectal cancer that the knockdown of CXCL1 would result in a decreased rate of glycolysis [20]. Our bioinformatics analysis shared similar findings of interaction between glycolysis-related gene PFKFB2 and CXCL1. The PFKFB family displays varying functions across different cancer types, with all linked to immune response. The expression of PFKFB2 was proved to be influenced in coordinating progression of gastric cancer and breast cancer. For validation, in SiHa and C33A cells treated with rCXCL1, PFKFB2 expression was upregulated in a concentration-dependent manner. In SiHa and C33A cells treated with M2φ-CM, PFKFB2 expression was increased and such increase was relatively reversed in M2φ-CM + CXCL1 Ab group. In SiHa cells, the promoted migration and invasion induced by rCXCL1 was restored by sh-PFKFB2 transfection. Similar rescue effect was also

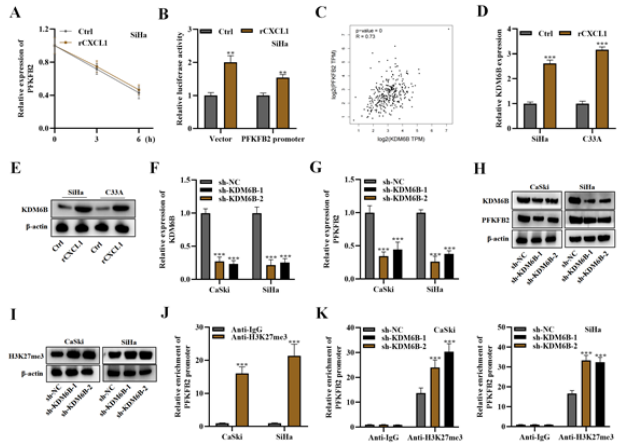

Fig. 4. ((A) Stability of PFKFB2 mRNA in SiHa cells from Ctrl/rCXCL1 group, detected at 0, 3 and 6 h via qRT-PCR. (B) Relative luciferase activity in SiHa cells transfected with Vector/PFKFB2 promoter and treated with Ctrl/rCXCL1. (C) Correlation between expressions of PFKFB2 and KDM6B, analyzed using GEPIA. (D-E) Relative expression of KDM6B in Ctrl/rCXCL1 group, detected by qRT-PCR and WB. (F) Interference efficiency of sh-KDM6B in SiHa and C33A cells. (G-H) Relative expression of PFKFB2 in SiHa and C33A cells transfected with sh-NC/KDM6B, detected by qRT-PCR and WB. (I) Relative expression of H3K27me3 in SiHa and C33A cells transfected with sh-NC/KDM6B, detected by WB. (J) Relative enrichment of PFKFB2 promoter in complex precipitated by anti-IgG/H3K27me3 from SiHa and C33A cells, assessed by ChIP assay. (K) Relative enrichment of PFKFB2 promoter in complex precipitated by anti-IgG/H3K27me3 from SiHa and C33A cells transfected with sh-NC/KDM6B, assessed by ChIP assay.

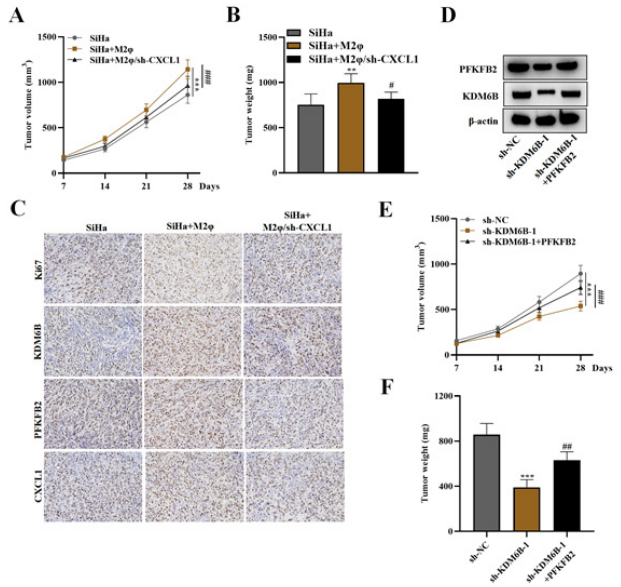

Fig. 5. (A) Tumor samples in vivo from SiHa, SiHa + M2φ and SiHa + M2φ/sh-CXCL1 groups. (B) Tumor volume and weight in vivo were sampled from SiHa, SiHa + M2φ and SiHa + M2φ/sh-CXCL1 groups. (C) Expression of KDM6B, PFKFB2 and CXCL1 in vivo sampled from SiHa, SiHa + M2φ and SiHa + M2φ/sh-CXCL1 groups, assessed by IHC staining. (D) Tumor samples in vivo from sh-NC, sh-KDM6B-1 and sh-KDM6B-1 + PFKFB2 groups. (E) Tumor volume and weight in vivo sampled from sh-NC, sh-KDM6B-1 and sh-KDM6B-1 + PFKFB2 groups. (F) Expression of KDM6B and PFKFB2 in vivo sampled from sh-NC, sh-KDM6B-1 and sh-KDM6B-1 + PFKFB2 groups, detected by WB.

observed in viability, levels of glucose uptake, lactate, ATP and ECAR. These results for the first time proved that CXCL1 regulated CESC progression via PFKFB2.

In 2019, KDM6B was identified to be involved in crosstalk between histone demethylation and hypoxic reprogramming in cancer metabolism [21], which was consistent with our bioinformatics findings. Moreover, KDM6B was confirmed to modulate the stability of nuclear β-catenin to regulate the M2 polarization of macrophages in breast cancer [22]. Our work shared similar mechanism in CESC. qRT-PCR and WB results showed that in vitro, KDM6B expression was upregulated by chemokine rCXCL1, and PFKFB2 expression was inhibited by sh-KDM6B. In vivo, the promoted tumor progression and expressions of KDM6B and PFKFB2 induced by transfected SiHa + M2φ were relatively restored by sh-CXCL1. Moreover, the inhibitory effect of sh-KDM6B-1 on tumor progression and expressions of KDM6B and PFKFB2 was restored in sh-KDM6B-1 + PFKFB2 group. These results suggested that CXCL1/KDM6B/PFKFB2 axis regulated CESC progression via interaction.

The protein encoded by KDM6B is H3K27me2 or H3K27me3 [23]. The trimethylation of H3K27 is an epigenetic modification that plays a crucial role in the regulation of chromatin structure and gene expression repression [24]. Additionally, this protein exhibits demethylation activity towards non-histone substrates, including retinoblastoma protein, thereby influencing various biological processes such as cellular differentiation and tumorigenesis [25, 26]. However, its regulatory network has not been fully explored, especially lacking in CESC. Our results showed that in SiHa and C33A cells transfected with sh-KDM6B, H3K27me3 expression was significantly increased. ChIP results indicated substantial enrichment of PFKFB2 promoter precipitated by anti-H3K27me3, which was further enriched in cells transfected with sh-KDM6B, suggesting KDM6B facilitated the binding of PFKFB2 promoter and H3K27me3, thus to inhibit the transcription of PFKFB2.

5. Conclusion

In conclusion, we determined the role of CXCL1 secreted by M2φ in CESC, which regulated metabolic reprogramming via KDM6B/PFKFB2 axis and provided valuable insights into the development of new therapeutic strategies for CESC targeting the tumor microenvironment.

Acknowledgements

This work was supported by Jiujiang Third People's Hospital.

Conflict of interests

The author has no conflicts with any step of the article preparation.

Consent for publications

The author read and approved the final manuscript for publication.

Availability of data and material

The data that support the findings of this study are available from the corresponding author upon reasonable request.

Authors' contributions

YJ conducted the experiments and wrote the paper; CL analyzed and organized the data; HL conceived, designed the study and revised the manuscript.

Funding

None.

References

1. He YH, Su RJ, Zheng J (2021) Detection of DKK-1 gene methylation in exfoliated cells of cervical squamous cell carcinoma and its relationship with high risk HPV infection. Arch Gynecol Obstet 304 (3): 743-750. doi: 10.1007/s00404-021-05982-3
2. Kruse AL, Grätz KW (2009) Cervical metastases of squamous cell carcinoma of the maxilla: a retrospective study of 9 years. Head Neck Oncol 1: 28. doi: 10.1186/1758-3284-1-28
3. Mantovani A, Sozzani S, Locati M, Allavena P, Sica A (2002) Macrophage polarization: tumor-associated macrophages as a paradigm for polarized M2 mononuclear phagocytes. Trends Immunol 23 (11): 549-555. doi: 10.1016/s1471-4906(02)02302-5
4. Boutilier AJ, Elsawa SF (2021) Macrophage Polarization States in the Tumor Microenvironment. Int J Mol Sci 22 (13). doi: 10.3390/ijms22136995
5. Nagarsheth N, Wicha MS, Zou W (2017) Chemokines in the cancer microenvironment and their relevance in cancer immunotherapy. Nat Rev Immunol 17 (9): 559-572. doi: 10.1038/nri.2017.49
6. Propper DJ, Balkwill FR (2022) Harnessing cytokines and chemokines for cancer therapy. Nat Rev Clin Oncol 19 (4): 237-253. doi: 10.1038/s41571-021-00588-9
7. Wu C, Ma C, Yuan J, Zhou P (2021) Exploration of potential therapeutic and prognostic value of CXC chemokines in cervical squamous cell carcinoma and endocervical adenocarcinoma based on bioinformatics analysis. Math Biosci Eng 18 (6): 8201-8222. doi: 10.3934/mbe.2021407
8. Liberti MV, Locasale JW (2016) The Warburg Effect: How Does it Benefit Cancer Cells? Trends Biochem Sci 41 (3): 211-218. doi: 10.1016/j.tibs.2015.12.001
9. Koppenol WH, Bounds PL, Dang CV (2011) Otto Warburg's contributions to current concepts of cancer metabolism. Nat Rev Cancer 11 (5): 325-337. doi: 10.1038/nrc3038
10. Liu Y, Ma L, Hua F, Min Z, Zhan Y, Zhang W, Yao J (2022) Exosomal circCARM1 from spheroids reprograms cell metabolism by regulating PFKFB2 in breast cancer. Oncogene 41 (14): 2012-2025. doi: 10.1038/s41388-021-02061-4
11. Ozcan SC, Sarioglu A, Altunok TH, Akkoc A, Guzel S, Guler S, Imbert-Fernandez Y, Muchut RJ, Iglesias AA, Gurpinar Y, Clem AL, Chesney JA, Yalcin A (2020) PFKFB2 regulates glycolysis and proliferation in pancreatic cancer cells. Mol Cell Biochem 470 (1-2): 115-129. doi: 10.1007/s11010-020-03751-5
12. Xun J, Gao R, Wang B, Li Y, Ma Y, Guan J, Zhang Q (2021) Histone demethylase KDM6B inhibits breast cancer metastasis by regulating Wnt/β-catenin signaling. FEBS Open Bio 11 (8): 2273-2281. doi: 10.1002/2211-5463.13236
13. Xun J, Du L, Gao R, Shen L, Wang D, Kang L, Chen C, Zhang Z, Zhang Y, Yue S, Feng S, Xiang R, Mi X, Tan X (2021) Cancer-derived exosomal miR-138-5p modulates polarization of tumor-associated macrophages through inhibition of KDM6B. Theranostics 11 (14): 6847-6859. doi: 10.7150/thno.51864
14. Jiang Y, Li F, Gao B, Ma M, Chen M, Wu Y, Zhang W, Sun Y, Liu S, Shen H (2021) KDM6B-mediated histone demethylation of LDHA promotes lung metastasis of osteosarcoma. Theranostics 11 (8): 3868-3881. doi: 10.7150/thno.53347
15. Sun H, Zhang X, Dai J, Pan Z, Wu Y, Yu D, Zhu S, Chen Y, Qin

T, Ouyang H (2020) Sodium lactate promotes stemness of human mesenchymal stem cells through KDM6B mediated glycolytic metabolism. Biochem Biophys Res Commun 532 (3): 433-439. doi: 10.1016/j.bbrc.2020.08.061

16. Sun F, Jie Q, Li Q, Wei Y, Li H, Yue X, Ma Y (2022) TUSC3 inhibits cell proliferation and invasion in cervical squamous cell carcinoma via suppression of the AKT signalling pathway. J Cell Mol Med 26 (5): 1629-1642. doi: 10.1111/jcmm.17204
17. De Filippo K, Dudeck A, Hasenberg M, Nye E, van Rooijen N, Hartmann K, Gunzer M, Roers A, Hogg N (2013) Mast cell and macrophage chemokines CXCL1/CXCL2 control the early stage of neutrophil recruitment during tissue inflammation. Blood 121 (24): 4930-4937. doi: 10.1182/blood-2013-02-486217
18. Li J, Wang S, Wang N, Zheng Y, Yang B, Wang X, Zhang J, Pan B, Wang Z (2021) Aiduqing formula inhibits breast cancer metastasis by suppressing TAM/CXCL1-induced Treg differentiation and infiltration. Cell Commun Signal 19 (1): 89. doi: 10.1186/s12964-021-00775-2
19. Kemp SB, Carpenter ES, Steele NG, Donahue KL, Nwosu ZC, Pacheco A, Velez-Delgado A, Menjivar RE, Lima F, The S, Espinoza CE, Brown K, Long D, Lyssiotis CA, Rao A, Zhang Y, Pasca di Magliano M, Crawford HC (2021) Apolipoprotein E Promotes Immune Suppression in Pancreatic Cancer through NF-κB-Mediated Production of CXCL1. Cancer Res 81 (16): 4305-4318. doi: 10.1158/0008-5472.Can-20-3929
20. Zhuo C, Wu X, Li J, Hu D, Jian J, Chen C, Zheng X, Yang C (2018) Chemokine (C-X-C motif) ligand 1 is associated with tumor progression and poor prognosis in patients with colorectal cancer. Biosci Rep 38 (4). doi: 10.1042/bsr20180580
21. Chang S, Yim S, Park H (2019) The cancer driver genes IDH1/2, JARID1C/ KDM5C, and UTX/ KDM6A: crosstalk between histone demethylation and hypoxic reprogramming in cancer metabolism. Exp Mol Med 51 (6): 1-17. doi: 10.1038/s12276-019-0230-6
22. Du L, Dai B, Liu X, Zhou D, Yan H, Shen T, Wang D, Tan X (2023) KDM6B regulates M2 polarization of macrophages by modulating the stability of nuclear β-catenin. Biochim Biophys Acta Mol Basis Dis 1869 (2): 166611. doi: 10.1016/j.bbadis.2022.166611
23. Romero OA, Vilarrubi A, Alburquerque-Bejar JJ, Gomez A, Andrades A, Trastulli D, Pros E, Setien F, Verdura S, Farré L, Martín-Tejera JF, Llabata P, Oaknin A, Saigi M, Piulats JM, Matias-Guiu X, Medina PP, Vidal A, Villanueva A, Sanchez-Cespedes M (2021) SMARCA4 deficient tumours are vulnerable to KDM6A/UTX and KDM6B/JMJD3 blockade. Nat Commun 12 (1): 4319. doi: 10.1038/s41467-021-24618-3
24. Liu X, Wang C, Liu W, Li J, Li C, Kou X, Chen J, Zhao Y, Gao H, Wang H, Zhang Y, Gao Y, Gao S (2016) Distinct features of H3K4me3 and H3K27me3 chromatin domains in pre-implantation embryos. Nature 537 (7621): 558-562. doi: 10.1038/nature19362
25. Nassiri F, Wang JZ, Singh O, Karimi S, Dalcourt T, Ijad N, Pirouzmand N, Ng HK, Saladino A, Pollo B, Dimeco F, Yip S, Gao A, Aldape KD, Zadeh G (2021) Loss of H3K27me3 in meningiomas. Neuro Oncol 23 (8): 1282-1291. doi: 10.1093/neuonc/noab036
26. Li Y, Goldberg EM, Chen X, Xu X, McGuire JT, Leuzzi G, Karagiannis D, Tate T, Farhangdoost N, Horth C, Dai E, Li Z, Zhang Z, Izar B, Que J, Ciccia A, Majewski J, Yoon AJ, Ailles L, Mendelsohn CL, Lu C (2022) Histone methylation antagonism drives tumor immune evasion in squamous cell carcinomas. Mol Cell 82 (20): 3901-3918.e3907. doi: 10.1016/j.molcel.2022.09.007